HYDROGEN EFFECTS ON CLEAVAGE FRACTURE IN FULLY PEARLITIC EUTECTOID STEEL

J.J. Lewandowski* and A.W. Thompson**

Blunt-notched bend bars of fully pearlitic AISI 1080 steel were tested in four-point bending at temperatures ranging from room temperature down to -125°C to determine the influence of microstructural parameters and dissolved hydrogen on the critical cleavage fracture stress. Failure in uncharged specimens was initiated by non-metallic inclusions or by fractured pearlite colonies. The cleavage stress, σ_F, in uncharged specimens decreased with increasing pearlite interlamellar spacing and was independent of the prior austenite grain size. Fracture initiation stresses were reduced by hydrogen, although fracture was not necessarily by cleavage. The degree of embrittlement decreased with decreasing test temperature. No measurable embrittlement was obtained at -125°C. The primary effect of hydrogen was to assist fracture nucleation ahead of a blunt notch.

INTRODUCTION

Orowan's (1) theory of brittle fracture was one of the earliest attempts at explaining cleavage fracture, where it was postulated that a critical value of tensile stress was required to produce cleavage. Furthermore, this "brittle fracture stress" was assumed to be relatively independent of temperature. Subsequent experiments on mild steel by Hendrickson et al. (2) and Knott (3) supported such an argument, and further indicated that some degree of localised flow or plasticity was required to initiate cleavage in mild steels. Additional work by Knott (4) and Curry and Knott (5) on cleavage fracture of relatively simple ferritic microstructures containing either grain boundary carbides or spheroidised carbides strongly suggested that, in those microstructures, the cleavage crack nuclei were individual cracked carbides. Knott (6) has suggested that the experimentally determined critical cleavage fracture stress, σ_F, represents the stress necessary to catastrophically propagate a cracked carbide into the surrounding matrix. While considerable work has focused on the fracture behaviour of relatively simple microstructures, less is known about cleavage fracture in more complicated microstructures. The initial part of this work focused on cleavage fracture in fully pearlitic microstructures

* Dept. Met. & Matls. Sci., Case Western Res. Univ., Cleve., OH.
**Dept. M.E.M.S., Carnegie-Mellon University, Pgh., PA

heat treated to vary microstructural features such as the pearlite interlamellar spacing, lamellar carbide thickness, and the prior austenite grain size.

A recent review of hydrogen embrittlement by Thompson (7) indicates that steels exposed to a hydrogen environment may exhibit "brittle" behaviour, often manifested by a loss in reduction of area or an increase in the amount of cleavage on a fracture surface. It is not certain whether the latter effect is due to an intrinsic effect of hydrogen on the strength of the iron lattice, as proposed by Troiano (8). Although hydrogen effects on ductile fracture modes have been fairly well characterised, less is known about how hydrogen may affect the more brittle modes of fracture. The goal of the present work was to determine the effects of dissolved hydrogen on cleavage fracture. Fully pearlitic eutectoid steel was chosen since it may fracture by cleavage at room temperature, thereby providing a convenient range of test temperatures over which to study hydrogen effects.

EXPERIMENTAL PROCEDURE

The chemical composition of the steel was analysed to be, in weight percent: 0.81 Carbon; 0.85 Manganese; 0.02 Sulphur; 0.018 Phosphorus; balance Iron. Specimen blanks were heat treated prior to machining. Austenitisation was conducted in dry argon at either 1000°C/3 hr. or 800°C/1 hr., followed by isothermal transformation in molten lead at either 675°C or 550°C. These heat treatments produced combinations of either a coarse (designated CG) or fine (i.e. FG) prior austenite grain size with either a coarse (i.e. CS) or fine (i.e. FS) interlamellar spacing. Table 1 lists the heat treatments and resulting microstructures. Additional microstructural details are provided by Lewandowski (9,10).

TABLE 1 Heat Treatments and Resulting Microstructures

Heat Treatment (microstructure)	Austenite Grain size (μm) ± 5μm	Pearlite Colony size (μm) ± 1μm	Pearlite Spacing (μm)
1000°C/3hr.,550°C/ 45 min. (CG/FS)	170	6.5	0.11
800°C/1hr.,550°C/ 45 min. (FG/FS)	30	5.5	0.125
1000°C/3hr.,675°C/ 45 min. (CG/CS)	170	6.0	0.25
800°C/1hr.,675°C/ 45 min. (FG/CS)	30	6.0	0.29

Tensile properties were obtained on ASTM E8 cylindrical tensile

specimens tested at: 23°C; -25°C; -75°C; -125°C. All tensile specimens were tested at an initial strain rate of 3.3×10^{-4}/sec.

The four-point bend specimens were dimensionally identical to that of Griffiths and Owen (11), and are shown in Fig. 1. Both single-notched and double-notched (9,10) (Knott (12)) specimens were tested to failure at constant displacement rates ranging from 0.0063 mm/min to 2.50 mm/min. The bend tests were conducted at the temperatures listed above, while cleavage fracture stresses were calculated with the Griffiths and Owen (11) finite-element analysis. Additional testing was conducted on bend bars machined to contain the following combination of root radii and flank angles; ρ = 1.0mm, $\theta = 45^{\circ}$; ρ = 1.0mm, $\theta = 90^{\circ}$; ρ = 0.25mm; $\theta = 90^{\circ}$. Cleavage fracture stresses on these specimens were calculated with the aid of the recently available finite-element analyses of Wall and Foreman (13) and Alexander et al. (14). During testing of the double-notched specimens, only one of the notched ligaments would fail. Fracture surfaces were examined on a Cambridge Instruments CAMSCAN 4 Scanning Electron Microscope (SEM). The unbroken "second" notch in such specimens represents a specimen unloaded immediately prior to catastrophic fracture. These unbroken ligaments were subsequently sectioned perpendicular to the bar thickness in an attempt to locate sub-notch cracks.

Hydrogen was introduced into the cylindrical tensile and notched-bend specimens by cathodic charging for 24 hours at 10 A/m^2 at room temperature in a 1N H_2SO_4 solution poisoned with 1 mg/liter As_2O_3. This should produce a flat concentration profile of hydrogen throughout the tensile specimens, and produce a similar profile ~ 3mm ahead of the notch root (9). Fully reversible embrittlement was obtained by charging at 10 A/m^2. Reversible embrittlement was defined as recovery of the uncharged values for reduction of area after baking precharged specimens for 24 hours at 150°C. Specimens tested at room temperature and -25°C were plated with Cd prior to testing in order to inhibit hydrogen egress. The remaining test conditions were identical to the uncharged tests.

RESULTS

The heat treatments described in Table 1 produced fully pearlitic-microstructures. Fig. 2 illustrates the mechanical properties obtained over the range of temperatures tested. The yield strength was controlled by the interlamellar spacing, S_p, while the prior austenite grain size primarily determined the reduction in area, as reviewed by Lewandowski and Thompson (15). The calculated values for the cleavage fracture stress obtained on uncharged specimens are plotted in Fig. 3. Neither changes in loading rate nor changes in bend bar geometry significantly changed the calculated values for σ_F. However, the data for σ_F appear to fall into two distinct groups. Fine pearlitic microstructures exhibited temperature- and notched-bar geometry independent values for σ_F, while the two coarse pearlitic

microstructures exhibited temperature dependent behaviour over a similar temperature range. The values for $\sigma_F \propto S_p^{-1}$ and were independent of the prior austenite grain size as shown by Lewandowski and Thompson (16,17).

Fracture initiation sites ahead of the notches could be located by tracing the cleavage river lines clearly present on the fracture surface. Cleavage fracture in approximately one-third of the uncharged specimens was triggered by a fractured non-metallic inclusion, as shown in Fig. 4. The inclusions responsible were observed to be in the size range 1-7 μm, which is orders of magnitude larger than an individual lamellar carbide. Cleavage facet sizes in all specimens scaled with the prior austenite grain size. No inclusions were found at the cleavage initiation sites in the remaining specimens (16,17). Sectioning the "second" notch revealed that fracture in these specimens was probably triggered by cracks associated with a pearlite colony or colonies, as shown in Fig. 5. Again, the fracture initiating flaw was much larger than the thickness of a single lamellar carbide. The size of cracks found ahead of the "second" notch varied from 2-35 μm depending upon the microstructure-test temperature combination (9,16,17).

Hydrogen precharged specimens typically exhibited reduced fracture stresses, as Fig. 6 illustrates for the fine pearlitic specimens. Similar behaviour was exhibited by the coarse pearlitic specimens. However, neither the yield strength or work-hardening exponent, n, were significantly affected by hydrogen. The degree of embrittlement for all four microstructures varied with test temperature. No embrittlement was obtained on any notched-bend specimen tested at -125°C. Although fracture stresses were clearly reduced by hydrogen, Fig. 7 shows that fracture surfaces of the hydrogen charged specimens were not necessarily 100% cleavage. Substantial amounts of fractographic plasticity were observed in tests conducted at room temperature and -25°C. Tests conducted at -75° and -125°C typically exhibited 100% cleavage.

Although the fractographic ductility exhibited by precharged bend specimens tested at room temperature and -25°C suggest that fracture initiation occurred at the notch root, sectioning the "second" notch provided clear evidence of sub-notch root fracture initiation. Fig. 8 shows that some radical cracking at the notch root accompanied the sub-notch root cracking. Cracking in the hydrogen charged specimens was primarily associated with pearlite colonies. Perhaps more importantly, fracture initiation of the type shown in Fig. 8 typically occurred markedly closer to the notch than the location of the peak stress (9). Little evidence of inclusion initiated fracture was obtained in hydrogen charged specimens.

DISCUSSION

The uncharged fine pearlitic specimens exhibited values for σ_F which were independent of test temperature, specimen geometry,

and loading rate, consistent with previous results obtained on mild steel (3-5). It appears that σ_F is primarily controlled by S_p and the lamellar carbide thickness, based on recent work (9,10,16,17) as well as that of Alexander (18) and Baker and Kavishe (19). One of the primary differences between the present work and previous work conducted on simple ferrite-carbide microstructures is the present observation that cleavage is initiated by features which are orders of magnitude larger than an individual carbide.

Values for the effective surface energies for cleavage, γ_{eff}, were calculated by using the Griffith-Orowan (20) equation combined with the size of initiating feature and the calculated cleavage fracture stress. The range of values calculated for γ_{eff}, 4-147 J/m^2, appeared to depend on both the microstructure and test temperature (9,17). In general, the calculated values for γ_{eff} increased with increasing test temperature and decreasing interlamellar spacing. Although it is generally felt that thermal fluctuations are insignificant in comparison to crack tip stresses at low temperatures (e.g. $< -75^{o}$C) (Knott (21)), the present work suggests that these effects may become important at temperatures near ambient, and hence may increase γ_{eff}. Additional discussion is provided elsewhere (9,17).

Uncharged coarse pearlitic specimens exhibited temperature dependent values for σ_F over a similar temperature range. This result has been reproduced in recent tests on steels of very similar composition (18,19). It has been suggested that such a result implies that fracture is nucleation controlled in coarse pearlite (19). However, arrested pearlite colony sized cracks ahead of the "second" notch in broken double-notched specimens have been observed (9,17). This strongly suggests that fracture nucleation is not the controlling stage in cleavage of coarse pearlite. Other possible reasons for this behaviour are presented elsewhere (9,17).

In discussing the hydrogen charged results, it must be remembered that the present work focused on reversible embrittlement effects. Hydrogen precharged specimens typically exhibited reduced fracture stresses, although the magnitude of embrittlement varied with both test temperature and microstructure. The temperature sensitivity of the hydrogen-induced reduction in σ_F and the return to the uncharged values for σ_F at -125^{o}C are suggestive of an inadequate mobility of hydrogen at the low temperatures. Although loading rates were adjusted to account for the reduced mobility of hydrogen at lower test temperatures (9), this was not effective in producing embrittlement at -125^{o}C. This suggests that some threshold level of hydrogen is required for fracture initiation. Furthermore, it indicates that the as-dissolved amount of hydrogen does not measurably affect fracture initiation.

The apparent anomaly in the observation of reduced fracture stresses accompanying an increase in the amount of fractographic plasticity in hydrogenated specimens can be rationalised as

follows. The presence of some critical amount of hydrogen clearly lowers the stress required to form fracture nuclei both at and ahead of a notch, as evidenced by the data presented in Fig. 7 combined with the metallographic evidence shown in Fig. 8. However, hydrogen-induced fracture is not necessarily cleavage at temperatures near ambient, but is a locally ductile type of fracture. This evidently means that hydrogen assists formation of the ductile fracture mode more than it can assist cleavage at temperatures near ambient. Subsequent crack propagation near ambient occurs in a locally ductile manner because the hydrogen-induced sub-notch cracks initiate at stresses which are insufficient to produce catastrophic failure. At lower test temperatures, the higher stresses at the initiation site are sufficient to produce catastrophic fracture upon fracture initiation.

The primary effect of hydrogen in the present work was to assist the formation of fracture nuclei ahead of a blunt notch. The observation that the location of hydrogen-induced cracking was not at the predicted peak stress location implies that some critical value of stress-strain product may be necessary for fracture initiation. The lack of embrittlement in specimens tested at -125°C further indicates that the as-dissolved concentration of hydrogen has no apparent effect on fracture initiation.

CONCLUSIONS

1. Cleavage fracture in uncharged fully pearlitic microstructures is controlled by the interlamellar spacing. Cleavage initiation was triggered either by non-metallic inclusions or by cracks associated with a pearlite colony or colonies. Cleavage initiating features were much larger than individual carbide thicknesses.

2. Hydrogen lowers the stress to form fracture nuclei, although subsequent fracture is not necessarily cleavage. At lower test temperatures, the reduced mobility of hydrogen decreases the degree of embrittlement.

3. The tests at -125°C indicate that the as-dissolved amount of hydrogen appears to have no measurable effect on fracture under notched-bend conditions.

ACKNOWLEDGEMENTS

The authors are grateful for many discussions with Drs. J.F. Knott, I.M. Bernstein and A.R. Troiano. Support for this work was provided by a Fannie and John Hertz Foundation Fellowship, with partial support by NSF grant # 81-19540.

REFERENCES

(1) Orowan, E., Trans. Inst. Engrs. Shipbuilders Scot. 89, 1945, pp. 165-215.

(2) Hendrickson, J.A., Wood, D.S., and Clark, D.S., Trans. ASM, 50, 1958, pp. 656-81.

(3) Knott, J.F., J.I.S.I., 204, 1966, pp. 104-11.

(4) Knott, J.F., J.I.S.I., 205, 1967, pp. 288-91.

(5) Curry, D.A. and Knott, J.F., Metal Sci., 12, 1978, pp. 511-14.

(6) Knott, J.F., Fundamentals of Fracture Mechanics, Butterworths, London, 1973, p. 178.

(7) Thompson, A.W., Mat. Sci. and Tech., 10, 1985, pp. 711-17.

(8) Troiano, A.R., Trans. ASM, 52, 1960, pp. 54-80.

(9) Lewandowski, J.J., Ph.D. Thesis, Carnegie-Mellon Univ., 1983.

(10) Lewandowski, J.J. and Thompson, A.W., in Fracture 1984 - Proc. 6th Intl. Conf. on Fracture - ICF6, (S.R. Valluri, et al., eds.), Pergamon Press, Oxford, Vol. 2, pp. 1515-24.

(11) Griffiths, J.R. and Owen, D.R.J., J. Mech. Phys. Sol., 19, 1971, pp. 419-31.

(12) Knott, J.F., J.I.S.I., 204, 1966, pp. 1014-21.

(13) Wall, M. and Foreman, A.J.E., Harwell Report No. 11620, 1985.

(14) Alexander, D.J., Lewandowski, J.J., Sisak, W.J. and Thompson, A.W., J. Mech. Phys. Sol., in press.

(15) Lewandowski, J.J. and Thompson, A.W., Met. Trans. A, March 1986.

(16) Lewandowski, J.J. and Thompson, A.W., Met. Trans. A, in press.

(17) Lewandowski, J.J. and Thompson, A.W., Acta Met., submitted.

(18) Alexander, D.J., Ph.D. Thesis, Carnegie-Mellon Univ., 1984.

(19) Baker, T.J. and Kavishe, F., Mat. Sci. and Tech., submitted.

(20) Orowan, E., Rep. Proc. Phys., 12, 1948, pp. 185-232.

(21) Knott, J.F. in Atomistics of Fracture, (R.M. Lantanison and J.R. Pickens, eds.), Plenum Press, N.Y. 1983, pp. 209-41.

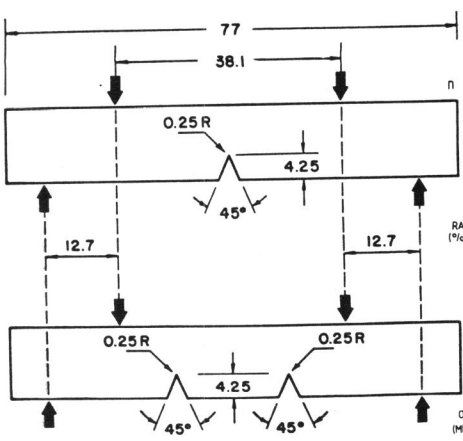

Fig. 1 Bend-Specimen Goemetries. Dimensions in mm.

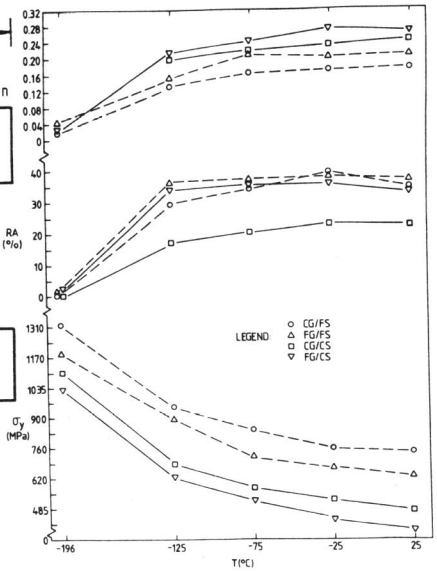

Fig. 2 Mechanical Properties

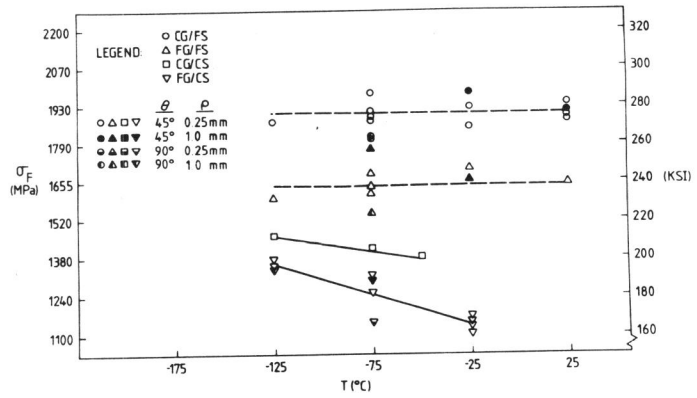

Fig. 3 Calculated Values for σ_F, Uncharged

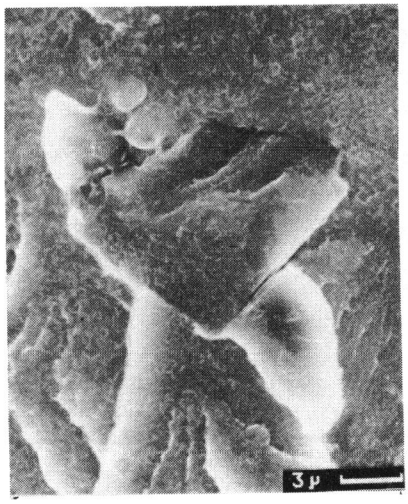

Fig. 4 Inclusion at Convergence of Cleavage River Lines

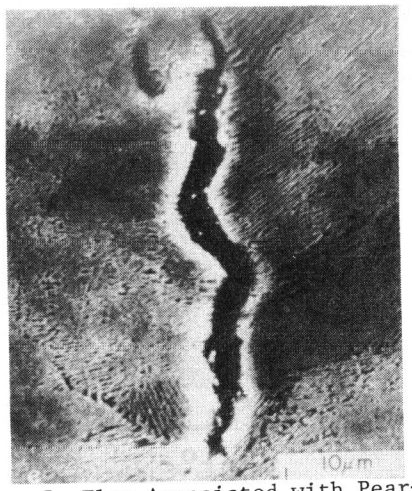

Fig. 5 Flaw Associated with Pearlite Colony Ahead of Notch

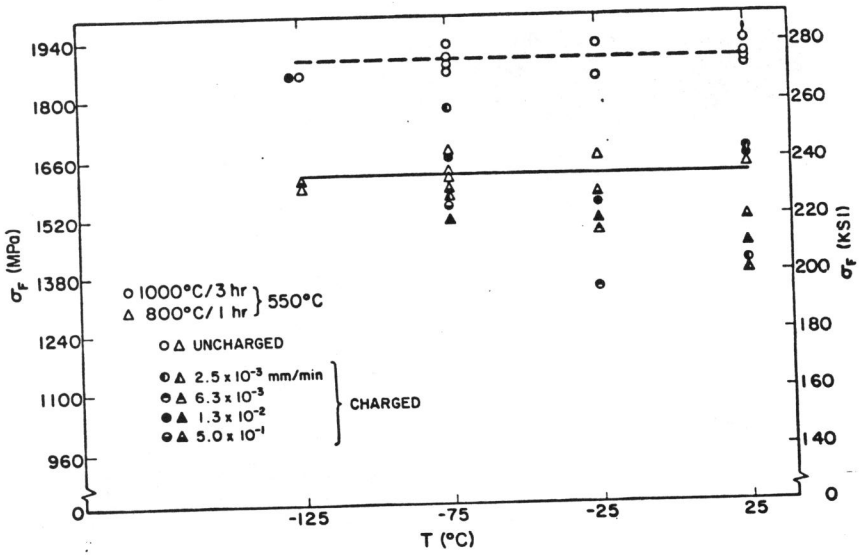

Fig. 6 Calculated Values for σ_F, Hydrogen Charged

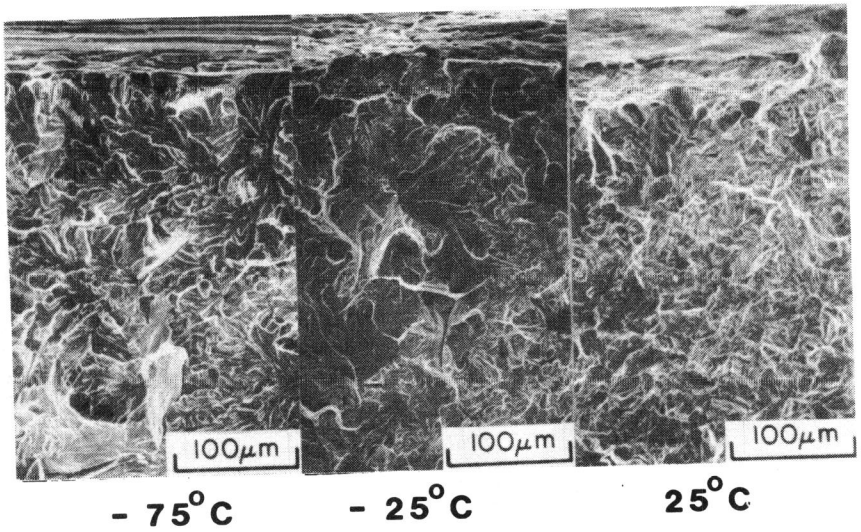

Fig. 7 Fracture Surfaces in Charged Specimens, Notch is at Top

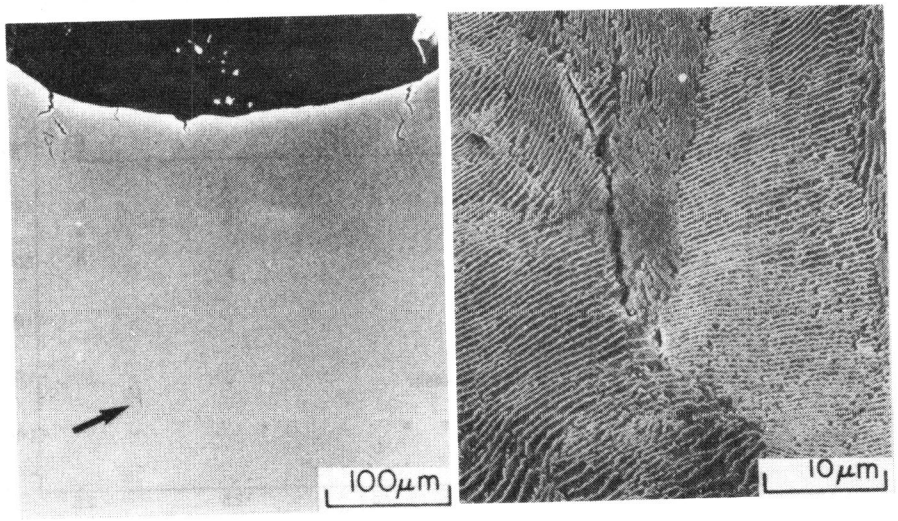

Fig. 8 "Second" Notch Showing Initiation Ahead of Notch In Hydrogen Charged Specimen